Early postglacial hunter-gatherers show environmentally driven þÿ f a l s e l o g i s t i c g r o w t h i n a l o w p r o d u c t i v i t y e n v i

Manninen, Mikael A.

2023-03-04

Manninen , M A , Fossum , G , Ekholm , T & Persson , P 2023 , ' Early postglacial þÿ h u n t e r - g a t h e r e r s s h o w e n v i r o n m e n t a l l y d r i v e n f a l s e l o g i s t i c g r o w t h i n environment ' , Journal of Anthropological Archaeology , vol. 70 (2023) , 101497 . https://doi.org/10.1016/j.jaa.2023.1

http://hdl.handle.net/10138/356208
https://doi.org/10.1016/j.jaa.2023.101497

Journal of Anthropological Archaeology 70 (2023) 101497

Contents lists available at ScienceDirect

Journal of Anthropological Archaeology

journal homepage: www.elsevier.com/locate/jaa

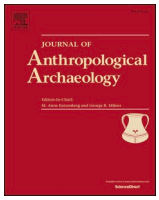

Early postglacial hunter-gatherers show environmentally driven "false logistic" growth in a low productivity environment

Mikael A. Manninen [a,*], Guro Fossum [b], Therese Ekholm [c], Per Persson [b]

[a] University of Helsinki: Faculty of Biological and Environmental Sciences, Past Present Sustainability Research Unit and Helsinki Institute of Sustainability Sciences, Helsinki, Finland
[b] Museum of Cultural History, University of Oslo, Norway
[c] Department of Archaeology and Ancient History, Uppsala University, Sweden

ARTICLE INFO

Keywords:
Logistic growth
Human population ecology
Population size
SPD
Prehistoric demography
Radiocarbon dates

ABSTRACT

Studies that employ probability distributions of radiocarbon dates to study past population size often use exponential increase in radiocarbon dates with time as a standard of comparison for detecting population fluctuations. We show that in the case of early postglacial interior Scandinavia, however, the summed probability distribution of radiocarbon dates has best fit with a S-shaped logistic growth curve. Despite the logistic growth model having solid grounding in ecological theory, we further argue that what our data indicate is not logistic growth in the population ecological sense but "false logistic" growth that mainly follows from climatic and environmental forcing. In the initial postglacial phase, 9500–7500 BCE, human settlement was located almost exclusively along the Scandinavian Atlantic coast and the use of the mountainous interior remained low. Thereafter the formation of separate inland adaptations resulted in population growth in tandem with increasing climatic warming and environmental productivity. Some millennia later, when environmental productivity started to decrease after the Holocene Thermal Maximum, hunter-gatherer population size in interior Scandinavia reached a plateau that lasted at least 2000 years. Lowering productivity prevented any population growth that would be detectable in the available archaeological record.

1. Introduction

The study of prehistoric demography through radiocarbon dates, i.e., the dates-as-data approach to human population dynamics, has seen a well-known boom in the last decades. Much of this research tests Summed Probability Distributions (SPDs) against a null model that assumes exponential increase in the number of radiocarbon dates with time. This approach stems from studies on Neolithic agricultural booms in Europe, according to which an exponential increase in the number of datable samples can be expected forward in time because of long-term population growth and increasingly better survival of dateable material in the archaeological record (Shennan et al., 2013, Timpson et al., 2014).

However, also other growth models have been increasingly tested to find the model with the best fit with radiocarbon dates in variable contexts (e.g., Goldberg et al., 2016, Bevan et al., 2017, Broughton and Weitzel, 2018, Solheim and Persson, 2018, Brown and Crema, 2019, Fernández-López de Pablo et al., 2019, Palmisano et al., 2021). Several of these authors have found that SPDs in their areas of study show a prehistoric population growth pattern suggesting logistic growth.

Logistic population growth, i.e., the Verhulst-Pearl logistic equation, is one of the most central models in population ecology (e.g., Verhulst, 1838, Kingsland, 1982, Begon et al., 1996: 246, Rockwood, 2006). The logistic population growth model assumes that population size is initially well below carrying capacity and therefore can grow unrestrained. As the area becomes more densely populated and population size approaches carrying capacity, the growth rate decreases and finally levels off, while population size becomes stable or alternates around a stable mean. This results in the S-shaped population growth curve characteristic for logistic population growth.

Tallavaara et al. (2018) identify three key environmental parameters in the ethnographic hunter-gatherer record, namely productivity, biodiversity, and pathogen stress, which globally drive hunter-gatherer population density. Looking at a more detailed set of climatic and environmental factors, Ordonez and Riede (2022) suggest that among the variables included in their analysis, effective temperature (ET), potential evapotranspiration, mean temperature of the coldest month, and

* Corresponding author.
E-mail address: mikael.manninen@helsinki.fi (M.A. Manninen).

https://doi.org/10.1016/j.jaa.2023.101497
Received 7 November 2022; Received in revised form 9 February 2023;
Available online 4 March 2023

probably also the mean temperature of the warmest month, were the most important limiting factors of hunter-gather population density in Early to Mid-Holocene interior Scandinavia.

According to Tallavaara and Jørgensen (2021; see also Jørgensen et al., 2022, Shennan and Sear, 2021, Tallavaara and Seppä, 2012): "*Long-term patterns in archaeological proxies may resemble, for example, logistic growth of saturating population size even though the pattern is actually a result of changes in the environmentally driven carrying capacity, where carrying capacity first increases and then stabilizes. Actual changes in the population size that follow a logistic growth model occur within time intervals that are usually beyond the resolution of archaeological proxies*." This is in accordance with observations of logistic growth in modern population ecological studies (Rockwood 2006: 46) and suggests that even if SPDs covering millennia-long time spans fit a logistic growth model, it is not because of true logistic growth in the population ecological sense, but rather because changes in biological productivity, and consequently in carrying capacity, happen to produce a growth curve similar in shape to the Verhulst-Pearl logistic equation. A mechanism that can be labeled "false logistic" growth.

Freeman et al. (2021), however, building on Malthus' notion that available resources limit population growth and Boserup's idea that gradual population growth causes population pressure leading to new forms of technology and/or social organization, advocate what they call the (Malthus-Boserup) MaB-ratchet model of long-term population growth among hunter-gatherers. In this model, when population density increases and approaches population saturation (i.e., carrying capacity), hunter-gatherers change their way of life as a response to the worsening state of the resource system. This development stimulates innovations that increase carrying capacity, and consequently also population growth. Population growth can therefore be considered both a catalyst and a result of cultural evolution (e.g., Boserup, 1965, Wood, 1998).

The MaB-ratchet model predicts a step-by-step population growth sequence for hunter-gatherers, where each step is signified by a certain new socio-technological system. Consequently, the model results in a series of population growth episodes that follow the logistic population growth equation. Freeman et al. (2021) argue that growth curves following the logistic model at multi-millennial scale can reflect real logistic growth episodes, as: "*Any population growth trajectory is composed of sequences of such trajectories at smaller scales*." As an alternative path following population growth, Freeman et al. (2021) note the possibility of situations in which humans are unable to create a new niche and thereby to increase carrying capacity, resulting in population saturation and consequently a lowered quality of life.

To study hunter-gatherer population dynamics in interior Scandinavia, we use a dataset of 639 radiocarbon dates representing 5500 years from Late Glacial ice sheet retreat to the introduction of agriculture to parts of the surrounding region. The dataset covers an extended period of continuous increase in environmental productivity that finally levels off causing human population growth to stall. We employ a model-fitting approach to test a set of growth models (exponential, logistic, linear, constant) against the distribution of our radiocarbon date dataset, consider the effect of increasing land area, and reconstruct effective temperature (ET) as a proxy for environmental productivity. We conclude that a model of logistic growth fits our early postglacial Scandinavian hunter-gatherer radiocarbon date dataset better than any of the other models we tested.

As Tallavaara and Jørgensen (2021) and Freeman et al. (2021) present differing approaches on how to interpret millennia-long S-shaped hunter-gatherer population growth curves, we discuss our results in the light of both views, tracking potential cultural and environmental drivers, and show that after the earliest use phase of the region, environmental limiting factors best explain the population dynamics observed in the SPD, while during the first phase also a cultural driver for the use of interior Scandinavia can be proposed.

2. Regional setting

Our study area is ca. 500,000 km^2 of interior Scandinavia south of 68 degreesN (Fig. 1). The first postglacial human dispersal into the Scandinavian Peninsula took place at the end of Younger Dryas, i.e., ca. 9500 BCE (Lohne et al., 2013, Manninen et al., 2021). However, since the center of the Scandinavian Ice Sheet covered interior northern Sweden, the study area remained uninhabited longer, as the last remnants of the ice sheet did not disappear before ca. 7700 BCE (Stroeven et al., 2016).

Geomorphology in the area was created by glacial and early postglacial processes, with large river and valley systems, lakes, alpine mountains and mountain plateaus, marshlands, and lowland plains. The Scandinavian Mountain range, with the highest peaks well over 2000 m above sea level, runs in a north–south direction through the Scandinavian Peninsula. The area east of the mountain range has a more continental climate with large seasonal variations in temperature and low precipitation, while areas west of the mountain range have a more maritime climate. Ecoclimatic conditions range from sub-arctic boreal forest in the lower-lying areas to treeless highland tundra (Bailey, 2014, Virtanen et al., 2016).

By *interior*, we mean the area that was 15 km or more from the seashore during its use in the Mesolithic. However, since the region has undergone considerable isostatic uplift since the beginning of deglaciation, these sites are currently found much further inland. Consequently, our radiocarbon date dataset derives from sites located from 65 to 1438 m above current sea level. It should be noted that these regional features increased the size of the habitable area during the studied period: the melting of land ice (last remnants of the Scandinavian Ice Sheet) increased the size of habitable area, while isostatic uplift also added to the areal growth.

Sites in the mountain region of SW Norway, dated to ca. 9200–8600 BCE (Bang-Andersen, 2012), and the Kangos site in northernmost Sweden from shortly after 8000 BCE (Ekholm, 2015), are the earliest archaeological evidence in the southern and northern extremities of the study area, respectively. These sites were near the retreating ice sheet margin at the time of their use.

The length of the growing season in interior Scandinavia, as indicated by effective temperature (ET = (18 W-10C)/((W-C) + 8), Bailey, 1960, Binford, 1980), that gives an indication of energy availability, is short. At present, ET values range from less than 10.00 in the high mountains to roughly 11.50 in the southernmost part of our study area (see Fig. 1), corresponding to a growing season between less than 40 to 120 days, depending on the location. The ET values indicate temperature-based boreal (ET is greater than 9.99 and less than 12.50) and polar (ET is less than 10.00) climate classes (Binford 2001, Tab. 4.02). There is near to non-existent agriculture in most of the area up until the present day.

3. Material and methods

The methodology used in this study rests on the premise of 'dates-as-data', meaning that more people will generate more (dateable) archaeological features (e.g., Rick, 1987, Gamble et al., 2005, Shennan and Edinborough, 2007, Riede, 2009, Surovell et al., 2009, Kelly et al., 2013, Shennan et al., 2013, Contreras and Meadows, 2014, Crombé and Robinson, 2014, Timpson et al., 2014, Williams, 2012, Brown, 2015, Tallavaara, 2015, Torfing, 2015, Crema et al., 2016, Palmisano et al., 2017, Roberts et al., 2018, Solheim and Persson, 2018, Fernández-López de Pablo et al., 2019, Jørgensen, 2018, Nielsen et al., 2019, Crema and Bevan, 2021, Solheim, 2020, Nielsen, 2021).

This approach, which uses Summed Probability Distributions (SPDs) of radiocarbon dates to reconstruct prehistoric population trends, has seen significant methodological improvements during the last decades that mitigate its much-debated biases, including sample size, investigation intensity, taphonomic loss, and problems in the calibration process (e.g., Tallavaara et al., 2014, Crema and Bevan, 2021, Crema,

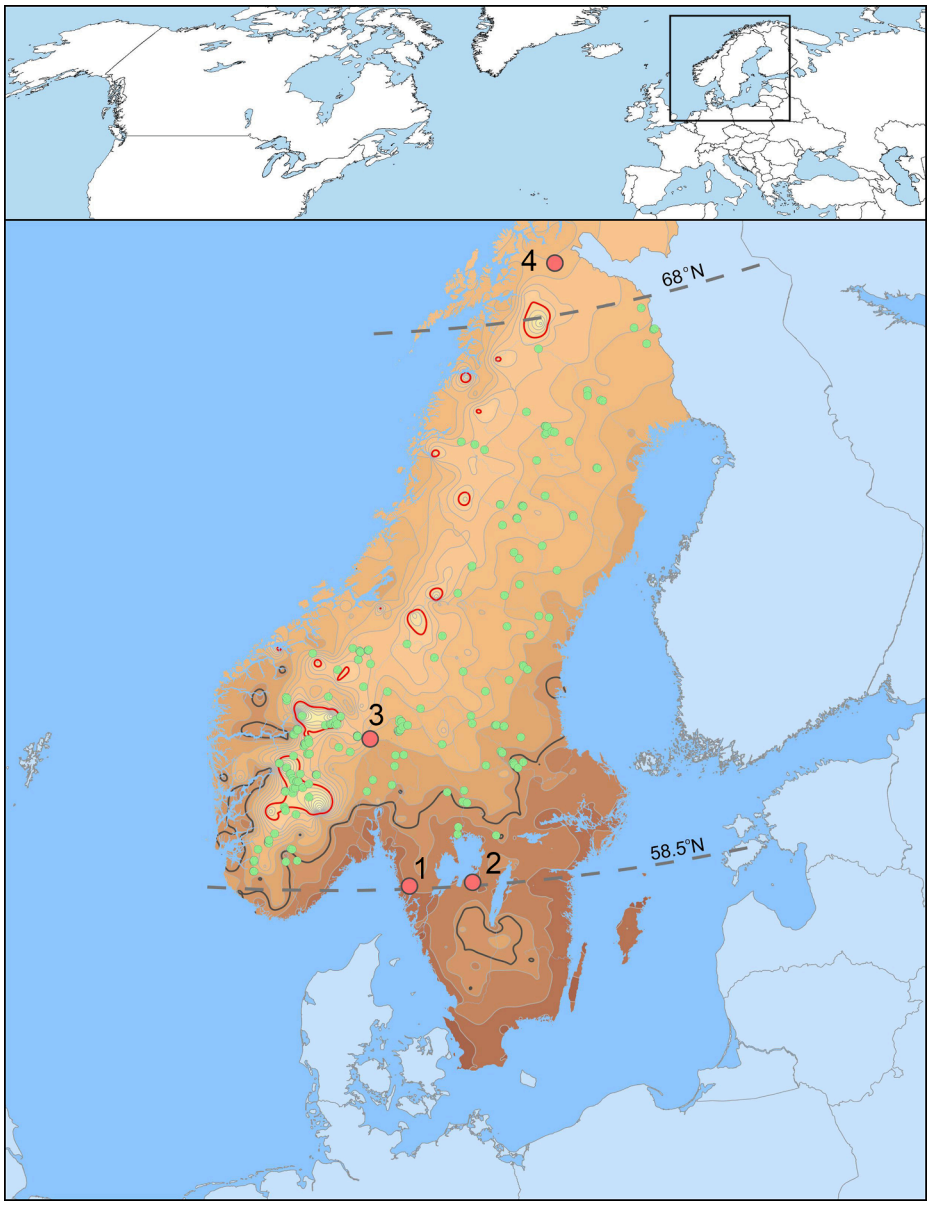

Fig. 1. The Scandinavian Peninsula and the studied sites. Small green dots indicate archaeological sites with radiocarbon dates used in this study. Larger red dots indicate locations from which data for the mean annual and effective temperature curves are derived: 1) Lake Trehörningen, 2) Lake Flarken, 3) Lillehammer, 4) Dividalen. Contour lines follow modern (1961–1990, Supplementary data S2) effective temperature (ET) values from warmer (darker) to colder (lighter). The black line indicates the ET 11.53 contour and the red line the ET 10.00 contour. Data from Aune (1993) and https://www.smhi.se/kunskapsbanken/klimat/normaler.

2022).

3.1. The radiocarbon date dataset

A dataset of 639 radiocarbon dates from between 9200 and 4000 BCE, deriving from 266 sites, is used in the study (Table 1 and Supplementary data S1). Datable archaeological material from the sites mainly consists of charcoal and calcined (burnt) bone. All radiocarbon dates are from archaeological contexts, mainly from development-led excavation projects and surveys. Practically all samples dated before 2005 are on charcoal. Approximately 1/3 of the dates were made by gas counting, while the rest are more recent accelerator (AMS) dates. The standard deviation varies accordingly, with samples dated in the 1900′s and early 2000′s (based on counting radioactive decay) having the highest values. Successively smaller standard deviation is present with more recently dated samples. Approximately 1/3 of the dates have a standard deviation of 55 years or less.

Table 1
The radiocarbon dates in the Mesolithic interior Scandinavia dataset according to sample material.

Sample material	N
Wood	5
Charcoal	400
Carbonized nutshell	23
Other carbonized organic remain	7
Pitch	2
Calcined bone	200
Unburnt bone	1
Antler	1
Total	**639**

It is often noted that radiocarbon dates on charcoal samples are prone to date human activity in forested environments unreliably. This is because charcoal in forest soils can derive from wildfires (see e.g., Couillard et al., 2019). The problem has traditionally been mitigated by dating relatively large charcoal pieces from selected contexts. Nevertheless, dates on calcined bone in the dataset (Table 2) are more securely linked to human activity than charcoal dates (e.g., Ekholm, 2015). The dates on calcined bone are AMS-dates on apatite (Lanting and Brindley, 1998, Lanting et al., 2001, see also van Strydonck et al., 2009, Agerskov Rose et al., 2019). Although they can be affected by old wood effect

Table 2
The radiocarbon-dated calcined bone samples in the dataset according to species.

Species		N
Alces alces*	Elk/moose	48
Rangifer tarandus	Reindeer/caribou	18
Sus scrofa	Wild boar	2
Castor fiber	Beaver	7
Lepus timidus	Hare	2
Homo sapiens	Human	1
Cervidae/Capreolinae	Deer	3
Mammalia	Mammalian	54
Esox lucius	Pike	1
Cyprinidae	Carps	1
Pisces	Fish	1
Indet.		63
Total*		**201**

* Including one antler axe

caused by the firewood used during the burning process (Olsen et al., 2013), and in some contexts dates on calcined bone have been found to be too imprecise for building decadal-to-centennial site chronologies (Crombé et al., 2021), in Fennoscandia burnt bone gives consistent and reliable results when dating sites (Oinonen et al., 2013, Ekholm, 2015, see also Naysmith et al., 2007), more accurate than charcoal samples, and are well suited for dates-as-data studies of population dynamics (Tallavaara et al., 2014). Dates on calcined bone and on charcoal in our dataset both fit well with the logistic growth model (Supplementary figure S7B).

3.2. Treatment of dates

All dates were calibrated using the *r-carbon* program (Crema and Bevan, 2021) and the IntCal20 calibration curve (Reimer et al., 2020). Dates were grouped per site using a 200-year bin size. The mean of all dates within the bin thus represents a 200-year period in the radiocarbon date SPD. Binning reduces the risk of wealth bias (i.e., over-representation) of certain sites and ensures that each site phase is equally weighted when generating the SPD (e.g., Timpson et al., 2014: 555, Crema and Bevan, 2021: 4-5). After binning, the radiocarbon dates in this study equal 440 bins. To avoid over-interpreting small features in the SPD, we also apply a running average of 200 years for the SPD curve (see e.g., Timpson et al., 2014: 550, Crema and Bevan, 2021: 4).

3.3. Monte Carlo simulation for the best fitting growth model

We use Monte Carlo simulation-based methodology (Shennan et al., 2013, Timpson et al., 2014) to test whether the features in the SPDs are statistically significant. However, our approach deviates from Shennan et al. (2013) in that, similarly to Fernández-López de Pablo et al. (2019), we test different population growth models to identify the overall best fit with our radiocarbon date dataset. Hence, the goal is not primarily to identify deviations from a fitted model but to test different growth models to determine which model has the best fit with the radiocarbon dates.

We use a random sample of dates from the tested model distribution and then back-calibrate the generated dates. This procedure produces sets of simulated radiocarbon dates that are attributed a random standard deviation from the pool of standard deviations in the actual radiocarbon dataset. The simulation allows the same date to be randomly generated more than once. Each simulation produces an SPD curve with the same number of simulated dates as there are empirical dates in the true radiocarbon date dataset but distributed according to a known model. The procedure is repeated 1000 times to give the span of random variation. The difference between the normalized true radiocarbon date SPD and the likewise normalized modelled SPD is detected by computing the area of the empirical distribution of radiocarbon dates that falls outside the 95 % probability of the modelled distribution. The smaller the computed area, the greater the overall fit between the model and the empirical SPD.

3.4. The tested population growth models

The exponential population growth model assumes a low starting population that starts to increase exponentially. The realistic maximal population growth for humans due to positive net reproduction is a few percentages per year. Even a low percentage means that the number of added people increases in tandem with population growth and will give a mirrored L-shaped exponential curve for population size vs. time (Malthus, 1798).

An exponential curve cannot, by definition, have a growth rate of zero, but growth rates very close to zero are possible. Such low growth rates mean a population growth that is close to linear growth, i.e., an addition of the same number of individuals each year regardless of population size and density. In such a situation the population growth measured as a fraction of total population will decrease with increasing population.

The logistic growth model assumes a limit of population density. Hence, the shape of the logistic population growth curve depends on two values: unrestricted growth rate (r) and carrying capacity (K). K is the environment's limit of population density in any given habitat. However, K can be expressed as a proportion of the start value, and then used in a logistic growth model. This gives the possibility to produce logistic curves and test for the best fit with the actual SPD without having an absolute value for K. By varying the r- and K-value, the best fit with the actual SPD can be sought.

The constant population model assumes no variables besides time and a constant population size. Consequently, only one model needs to be tested. Due to the drastic environmental changes at the end of the last glacial period, a constant population during the Early Postglacial in our study area is unlikely, since in the earliest phases the population size was zero or close to zero. However, a rapid initial dispersal would be close to instant population growth, which, if combined with population control, could in principle match a constant population model.

3.5. Land area increase

Since the size of the study area grew with time due to ice sheet retreat and isostatic uplift, there is a possibility that it is reflected in population size even when population density remains constant. We therefore use reconstruction maps of land area, ice sheet size, and sea-covered area, that show changes in these variables at 100-year intervals (Påsse and Andersson, 2005, Daniels, 2010, Påsse and Daniels, 2011) to calculate the areal growth of the Scandinavian Peninsula per timeslot on these maps. This is done by calculating the number of pixels classified as land per map. We evaluate the effect of increasing land area size on the radiocarbon dataset by comparing the increase in the land area against the radiocarbon date SPD. If population density is assumed to be constant, total population size, and consequently the number of radiocarbon dates, should increase with land area.

3.6. Temperature reconstruction and environmental contextualization

To contextualize the population growth in relation to changes in environmental conditions through time, we use modelled Holocene temperature reconstructions (deviation from modern temperature (°C) of the warmest (W) and coldest (C) months) for southern and northern Norway (Lilleøren et al., 2012). We calculate effective temperature (ET = (18 W-10C)/((W-C) + 8), Bailey, 1960, Binford, 1980) estimates ca. 8000–4000 BCE for the southern and northern parts of the study area using the modelled regional deviations from current temperature in southern and northern Norway, compared against the average modern (1961–1990) January and June temperature at the Dividalen

meteorological station (228 m asl, northern Norway; Aune 1993) and three Lillehammer weather stations (226–271 m asl, Lillehammer-Satherengen, Lillehammer II & Lillehammer III; Aune 1993). In addition, we use pollen-based temperature reconstructions from Lake Trehörningen (Antonsson and Seppä, 2007) and Lake Flarken (Seppä et al., 2005) that also cover the beginning of the Holocene. These lakes are the northernmost available covering the studied timespan even if located south of our study area (Fig. 1).

The lack of high-resolution data on precipitation during the Early to Middle Holocene in interior Scandinavia prevents reliable calculations of net aboveground productivity in the studied timeframe. We therefore use ET also as a proxy value for relative productivity. Biological diversity and productivity get gradually lower with higher latitudes and lower temperatures. A bottleneck in net aboveground productivity is reached at ca. 55th parallel north or ET 11.53, after which an accelerating reduction in productivity occurs (Binford, 2001: 265p).

A benefit of using ET as a proxy for environmental conditions is that data collected from the global ethnographic record suggest that many features in hunter-gatherer subsistence strategies and social organization are predicted by effective temperature (Binford, 1980, 2001, Kelly, 2013, Johnson, 2014). This makes it possible to predict hunter-gatherer behavioral patterns and other environmental limiting factors based on ET values. Effective temperature is also modelled among the most important limiting factors for human population density in our study area during Early Holocene, while the others include mean temperature of the coldest month, potential evapotranspiration, and probably also mean temperature of the warmest month (Ordonez and Riede, 2022). Of these the mean temperatures of the coldest and warmest months are built into and correlate with ET.

4. Results

4.1. Radiocarbon date summed probability distribution

The SPD for all radiocarbon dates in the dataset is shown in Fig. 2, as well as the effect of binning those dates that show similar age and derive from the same site. As the dataset has only a few sites with a large set of dates from the same use phase, the binning of dates causes only minor changes in the curve.

4.2. Models of population growth

Fig. 3 shows the differences between the radiocarbon date SPD and the different population growth models (for more details, see Supplementary text 1). The constant population model does not fit the actual SPD well (Fig. 3A). For roughly the first half of the studied period the population size indicated by the SPD is lower than this model would suggest, while for the second half of the period it is higher. The constant population scenario is therefore very unlikely, as it fails to detect the ca. 2500 years long period of initial population increase.

Fig. 3B shows a modelled 1% annual exponential growth curve compared with the radiocarbon date SPD. Even if the world population has been growing at a rate higher than 1% for more than a century now, such an increase is impossible for long. A 1% growth rate gives a doubling time of approximately 70 years. With a modelled start of just one couple, already after 1300 years the first million is reached, which is then doubled only 70 years later.

By comparing the radiocarbon date SPD with curves representing diverse exponential growth rates, it can be shown that the fit with the model is increasingly better with successively lower growth rates (Supplementary text 1). In Fig. 3C a 0.3% annual growth is shown as an example. The lowest growth (Fig. 3D) gives a virtually straight line from the initial population to a maximum at the end of the studied period. These very low growth rates give the best fit among all possible exponential growth scenarios when compared to the actual SPD. This is close to linear population growth, i.e., adding the same number of individuals per year for the whole period. Yet, despite being the best among the exponential models, the fit is not much better than the constant population model. The addition of an equal number of people each year, i.e., linear population growth, is also unlikely from a theoretical point of view, as no known mechanism could explain such a growth pattern.

Compared to the other models we tested, the logistic model results in realistic population growth scenarios and has the best fit when compared to the radiocarbon date SPD (Fig. 3E-G). In the logistic growth model, maximum growth takes place only when population size is much lower that carrying capacity, while the growth rate decreases as population size starts to approach carrying capacity. The best fit with the radiocarbon date SPD is achieved with unconstrained annual growth rate (r) of 0.2% combined with a K-value of 100 times the starting population. Starting with 40 individuals at 9500 BCE the population would increase, according to the model, to 4000 individuals at 6500

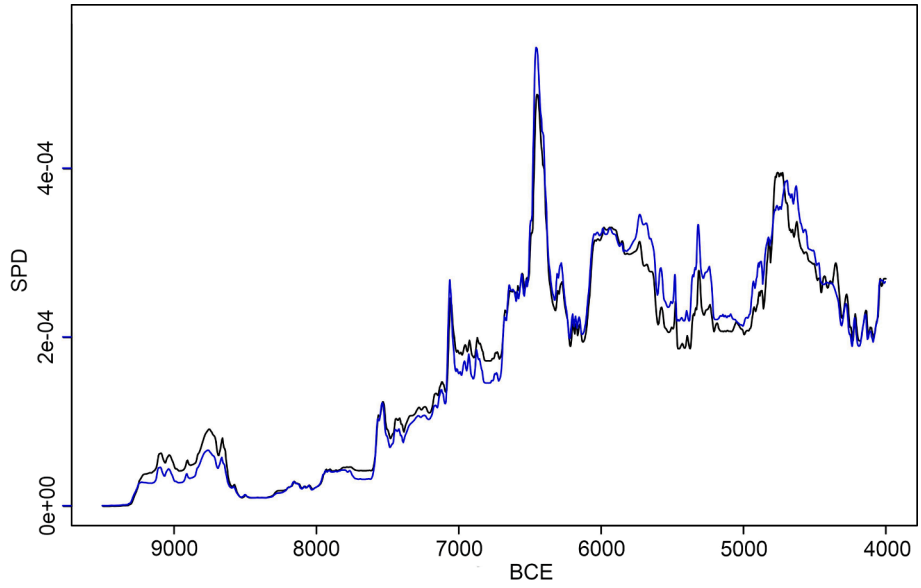

Fig. 2. Summed Probability Distribution of the radiocarbon dates and the effect of binning. The black curve shows the raw data without binning and the blue curve the effect of binning dates from the same site in 200-year bins. The area below both these curves is 1 (cf. Figure S1).

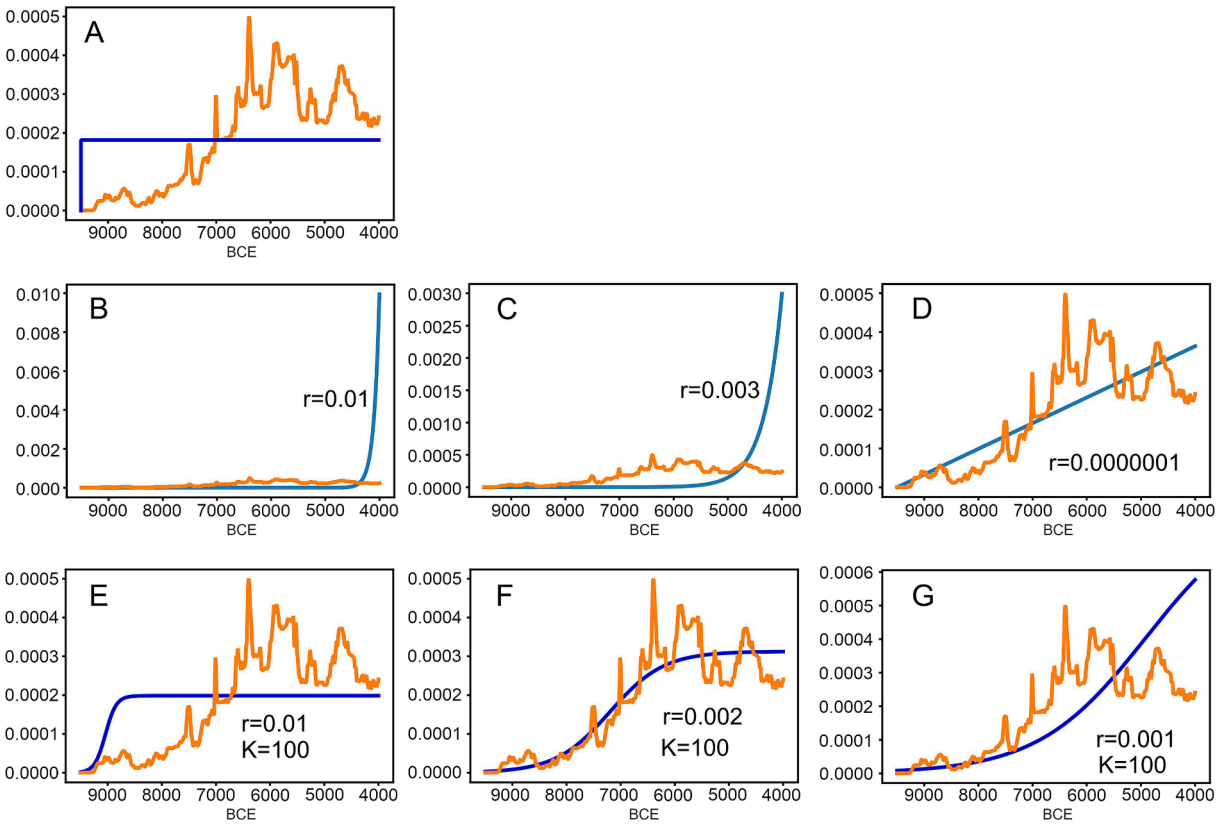

Fig. 3. Examples of different models for population growth fitted against the actual distribution of radiocarbon dates in this study: A) constant, B-C) exponential, D) linear (exponential), and E-G) logistic. The blue lines indicate a tested model while the orange line is the SPD. The examples represent the different growth models described in the text with different combinations of growth rate (r) and carrying capacity (K). The r = 0.002/K = 100 logistic model (F) has the best fit with our radiocarbon date dataset.

BCE, after which the population would stay constant for the following 2500 years covered by our dataset. An alternative start with 1000 individuals would end with a population of 100,000. Although we have no means of evaluating accuracy between such alternative scenarios, it can be noted that a population exceeding 100,000, in our case more than 10 persons per 100 km^2 for the whole area, is not realistic when compared to known hunter-gatherer population densities in tundra and boreal forest environments (Binford, 2001: 5.10, Kelly, 2013: tab.7–3, Zhu et al., 2021).

An unconstrained growth rate of 0.2% may sound high when compared with, for instance, results presented by Zahid et al. (2016) that show average annual growth of 0.04% among hunter-gatherers. The

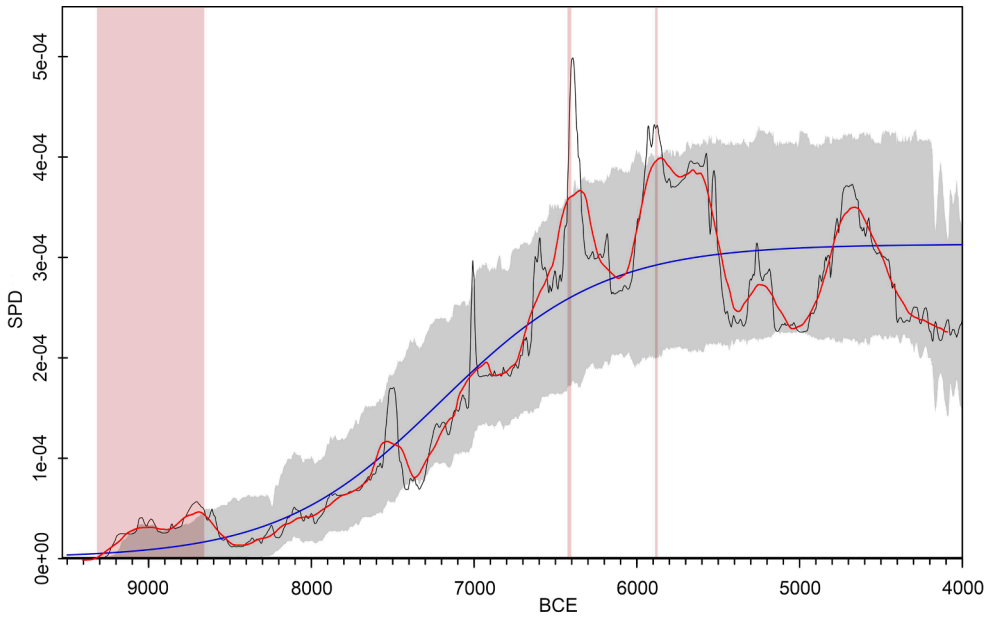

Fig. 4. SPD for all radiocarbon dates in 200-year-bins (black line) and the best fit logistic model (blue line). The grey area is the outcome of 1000 simulations with the same number of radiocarbon dates and the same standard deviation values as in the actual dataset but randomly distributed according to the model. The red line shows the SPD as a 200-year running average. The red areas show the two periods in which the actual dates give a significantly higher signal than a random distribution from the model.

difference stems from the fact that in logistic growth models annual growth rate is given as the maximum value possible when population size is well below carrying capacity. As population grows, the annual growth rate decreases, and becomes zero when carrying capacity is reached. With an unconstrained growth rate of 0.2%, the average annual growth rate in the studied timeframe is 0.018% (i.e., an increase of 100 times starting population in 5500 years). It should also be noted that an annual growth of 0.2% for short periods is well in agreement with figures for recent hunter-gather population growth, and periods of rapid annual prehistoric hunter-gatherer population growth, in other parts of the world (see Kelly et al., 2013, Tallavaara and Jørgensen, 2021).

The best fit of the logistic growth model with the radiocarbon date SPD (Fig. 4), can be further demonstrated by splitting the dates into two distinct data sets, e.g., one with the dates on charcoal and a second with the dates on calcined bone. Both datasets show an overall correspondence with this logistic model (Supplementary text 2, figure S7B), which is a good indication that the results are robust. To further test the robustness of the logistic model with our dataset, we summed the number of sites with radiocarbon dates in each 200-year interval to see if a similar pattern would emerge as in the SPD (Supplementary text 2, figure S6). This is, in fact, the case: before ca. 6500 BCE each 200-year interval shows 1–5 sites, which turns into 25–35 sites per 200-years after 6500 BCE.

Between ca. 9300 and 8700 BCE the SPD shows a large positive deviation from the logistic model. This deviation seems to indicate a much larger inland population during the pioneer human dispersal into the area than predicted by the model. However, most of these dates (24 of 25 dates in 10 bins) derive from sites around two lakes close to the Atlantic coast in the mountain region of south-western Norway (Bang-Andersen, 1990, Tørhaug and Åstveit, 2000). These sites are commonly considered logistic reindeer hunting camps utilized by Early Mesolithic coastal groups (e.g., Bang-Andersen, 2012, Breivik and Callanan, 2016). Furthermore, these sites were the first Early Mesolithic sites discovered in the Norwegian mountain region, and the large number of radiocarbon dates is, at least in part, a result of high research interest. Therefore, we do not consider this deviation to indicate a period of high population density in the interior, but instead suggest that constant low population suggested by the model is closer to the real situation.

Short but significant positive deviations from the model can also be detected at approximately 6400 BCE and 5900 BCE. These two deviations, however, nearly disappear when the running average is used instead of the raw SPD curve. The first clear dip in the SPD coincides with the 8.2 ka climate event, one of the best-known cold periods in the early Holocene (Alley et al., 1997), and documented also in Scandinavia (Nesje and Dahl, 2001). This event has been held responsible for cultural changes and population decrease in different parts of Fennoscandia (e.g., Manninen et al., 2018, Jørgensen et al., 2022, Schulting et al., 2022). A second dip in the SPD starting at approximately 5600 BCE and continuing up to 5000 BCE can also be observed but does not correlate with lowering ET. Both of these fluctuations, however, remain within the 95% confidence interval of the logistic population model and are not statistically significant.

4.3. *Effective temperature*

Change in ET over time (Fig. 5A) shows a rapid rise in the northern part of the study area between ca. 7800–7600 BCE, continued by a moderate rising trend reaching its maximum (ET 11.34) at ca. 4850 BCE, after which ET starts to decrease. The Early to Middle Holocene warming trend is interrupted by two periods of rapid cooling, the first culminating ca. 7400 BCE (ET 10.85) and the second ca. 6200 BCE (ET 10.96). In the south, a continuous gradually rising trend in ET is interrupted by a cooling period beginning at ca. 6600 BCE and culminating ca. 6150 BCE (ET 11.45). The rising ET reaches its maximum around 5600 BCE (ET

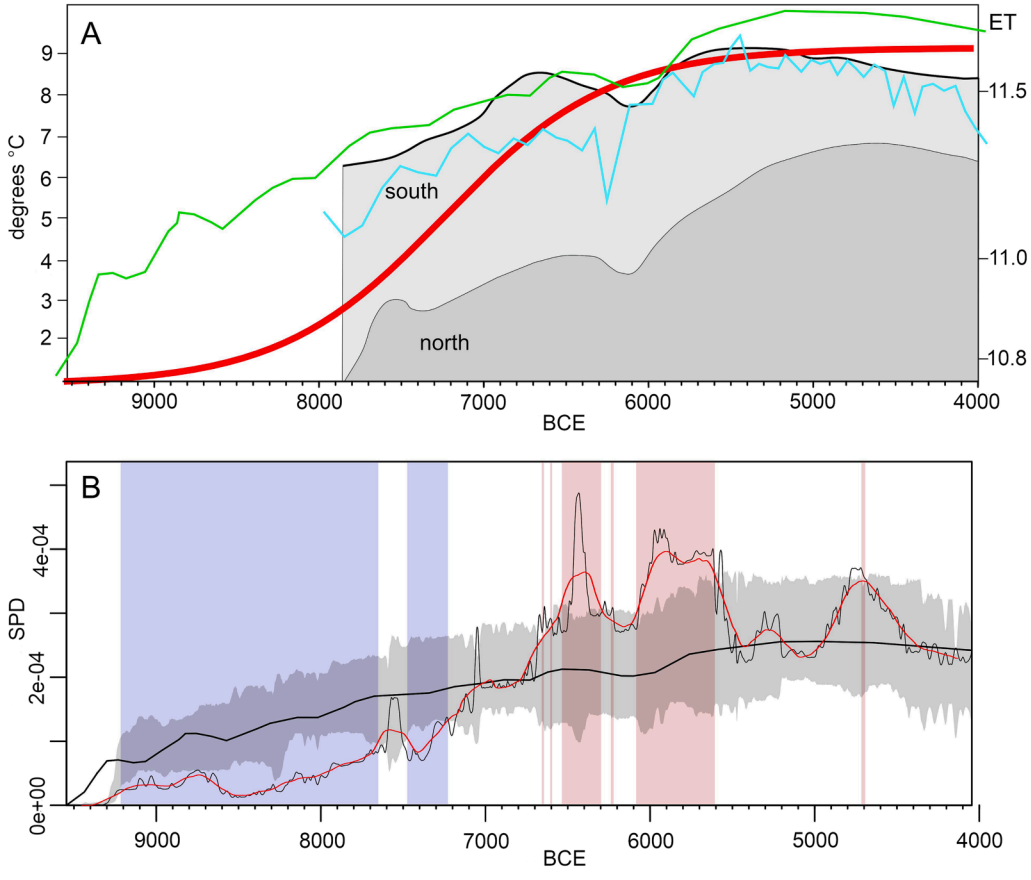

Fig. 5. A) Temperature reconstructions compared to the best fit logistic model (red line). Gray areas with black lines = changes in modelled effective temperature (ET) over time in Dividalen (north) and Lillehammer (south) in our study area (scale to the right). Holocene annual mean temperatures at Lake Trehörningen (green curve; after Antonsson and Seppä, 2007), and Lake Flarken (blue curve, after Seppä et al., 2005). B) The annual mean temperature reconstruction from Lake Trehörningen (thick black line) used as model and compared to the SPD (thin black line). The grey area indicates the outcome of 1000 simulations with the same number of radiocarbon dates as in the actual dataset and the same values for standard deviation, but randomly distributed according to the model. The red line shows the SPD as a 200-year running average.

11.6) and starts to slowly decrease after ca. 5400 BCE. These ET values correspond to initial polar (ET less than 10.00) and later boreal (ET 9.99–12.50) climates in the low-lying parts of the study area. The highest ET values in each area are indicative of the Holocene Thermal Maximum.

Although our ET values are based on modelled temperatures of the coldest and warmest month and therefore should not be considered exact, they nevertheless indicate that even the low-lying areas in the southern part of the study area during 9500–4000 BCE were at or below the "subpolar bottleneck" (11.45 to 11.60 degrees ET, Binford 2001: 265p), below which net aboveground productivity is reduced sharply, while the reduction accelerates as ET further decreases. Relative differences in ET between higher and lower-lying parts of the study area can be assumed to have been analogous to the present situation. The pollen-based reconstructions of annual mean temperature (Fig. 5B) are in good agreement with the modelled ET-values and show the early postglacial temperature rise. The best fit logistic growth model shows a general agreement with both the annual mean temperature and ET curves. Although we do not have modelled ET values for the earliest ca. 1700 years of human dispersal into the area, it can be extrapolated from the pollen-based proxies that ET was lower in the period 9500 to 7800 BCE than after.

4.4. Population vs. Land area increase

The increase in land area is presented in Fig. 6A and compared with modelled population growth, i.e., the logistic growth model with the best fit. It shows a long period during which the land area increased without corresponding population growth. In Fig. 6B, the increase in land area is compared with the radiocarbon date SPD. This shows a long period of "underpopulation" when the actual SPD is significantly lower than predicted by the increase in land area, and, due to the symmetry in the method, is followed by a period of "overpopulation". Therefore, the increase in the interior land area during the studied period does not seem to be of any major importance in explaining population size when using a low-resolution archaeological population proxy.

An initial rapid increase in land area due to the retreat of glaciers ended rather abruptly ca. 7500 BCE, after which there was only a slow increase due to general land upheaval. This increase in land area is not followed by an increase in human population. Even if the productivity per area unit in the initial phase most likely was low (see Tallavaara et al., 2014, Ficetola et al., 2019), all other things being equal, the total biological productivity of the Scandinavian inland region should increase in tandem with its size. Despite this, the inland population was low until 8000 BCE. If the SPD and the fitted logistic growth curve are compared to available land area, a drastic decrease in inland population density can be observed (Supplementary text 3).

5. Discussion

The Early to Middle Holocene warming trend observed in the pollen-based proxies just south of the study area, as well as in the modelled ET curves for the study area, coupled with the marked initial land area growth, suggest continuously increasing bioproductivity from ca. 9500 BCE until ca. 6000 BCE. Nevertheless, despite the warming trend and the Holocene Thermal Maximum occurring in the studied period, ET in the area always stayed low, suggesting low floral and faunal diversity (Fischer, 1960). ET was almost categorically below the subpolar bottleneck (ET 11.53, Binford, 2001), under which productivity and biomass rapidly drop off with lowering ET values, thus confirming that our radiocarbon dataset, as expected, derives from low productivity conditions.

From the ethnographic hunter-gatherer data it can be argued that such low ET values meant that hunter-gatherers in the area had low population density due to low trophic efficiency (Johnson, 2014, Zhu et al., 2021), were largely dependent on terrestrial hunting of large herbivores and, where possible, to a degree also fishing (Binford, 2001: 368, Kelly 2013: 46), had large territories (e.g., Kelly, 2013: 95), made long residential moves that on average grew in distance as ET decreased (Kelly, 1983, Binford, 1980, 2001, Johnson, 2014), were largely dependent on stored food, and procured a large percentage of their annual food supply during short segments of the growing season

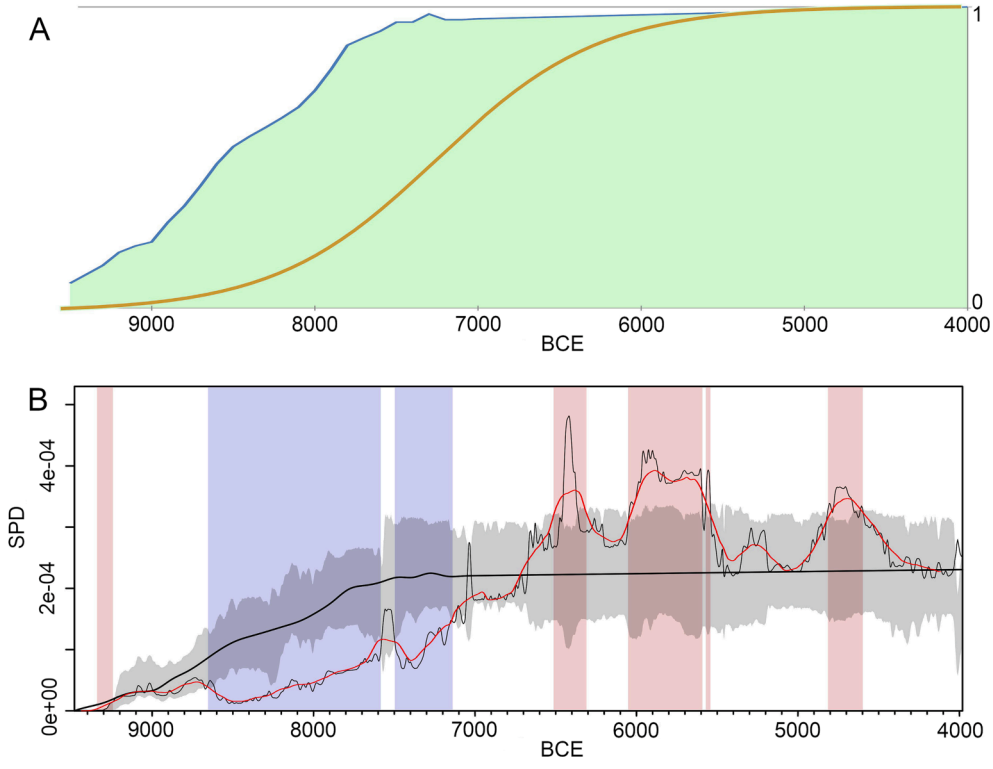

Fig. 6. A) The increase in land area in the investigated area compared with the best fit logistic growth model. The increase in land area is mostly due to the retreat of the ice sheet but after ca. 7500 BCE it is only the land upheaval that contributes. B) The land area used as a model (thick black line) against the SPD (thin black line). The grey area is the outcome of 1000 simulations with the same number of radiocarbon dates as in the actual data set and the same values for standard deviation, but randomly distributed according to the model. The red line shows the SPD as a 200-year running average. Land area size based on reconstruction maps by Påsse and Andersson (2005).

(Binford, 2001: 268).

Our results also show that a logistic population growth model with a unrestricted annual population increase of 0.2%, and a stabilization of population at 100 times the initial size, has the best fit with our radiocarbon data. We find it unlikely that a growth curve following the logistic equation can be explained by factors related to the survival of charcoal in the archaeological record (see Surovell et al., 2009, Shennan et al., 2013, Timpson et al., 2014). Instead, we argue that this represents an average of interior Scandinavian population development 9500–4000 BCE.

Considering the two alternative explanations for millennia-long S-shaped hunter-gatherer population growth curves, i.e., the Freeman et al. (2021) MaB-ratchet model in which episodes of logistic growth are explained by socio-technological changes that take place in face of population saturation to bypass resource depletion, and the notion by Tallavaara and Jørgensen (2021) that environmentally driven carrying capacity, that first increases and then stabilises, can produce a population growth curve that resembles logistic growth, we will next scrutinze the long period of "underpopulation" ca. 9500–7500 BCE when the actual SPD is significantly lower than predicted by the increase in land area, the period of rapid growth after ca. 7500 BCE, and the period of population saturation from ca. 6000 BCE onwards.

5.1. The beginning of Scandinavian inland settlement

According to isotope analysis, the Scandinavian west coast was populated since 9500 BCE by specialized groups with maritime adaptation and a close to 100% marine diet (Skar et al., 2016, Boethius and Ahlström, 2018). Also hunting of land mammals did take place, while bone and antler were used for tools and fishing equipment (Mansrud and Persson, 2018). Nevertheless, it was the availability of marine resources that seems to have determined population size, as land mammals were only a very minor part of the diet. Despite the constant increase in land area ca. 9500–7500 BCE (Fig. 6), population size in the interior did not grow accordingly at this stage, resulting in decreased population density (Supplementary text 3, figure S8).

The earliest inland settlement is found in the western Scandinavian mountains around 9200 BCE (Bang-Andersen, 1990, Tørhaug and Åstveit, 2000). The western Scandinavian coastal sites have a high proportion of artifacts made of cretaceous flint, a raw material available locally only in the coastal region, while site assemblages at contemporary inland sites in the adjacent interior region are also dominated by flint (Bang-Andersen, 2013, Breivik and Callanan, 2016), suggesting that coastal and inland sites were parts of the same settlement system. The situation changes after ca. 8000 BCE when local lithic raw materials, such as jasper and quartzite, start to dominate site assemblages in the interior (Melvold, 2011; Damlien and Solheim, 2018). Considering that the use of flint continues in the coastal region, this change in raw material economy, alongside associated changes in housing constructions and increasing variability in site locations in the interior, signifies a break in the earlier coast-inland mobility pattern. Together with the continuous specialization in marine resource use along the coast, these changes reflect the forming of a separate population with year-round inland adaptation from ca. 8000 BCE (Boaz, 1999, Damlien and Solheim, 2018).

If we assume that during ca. 9500–8000 BCE the use of the interior was a minor and opportunistically utilized part of the coastal adaptation, the increase in inland bioproductivity could not be used to its full potential. Especially since the strong maritime orientation in subsistence economy required precence at the coast for most of the year. It was only when an interior population with its own social, technological, and subsitence organization started to develop ca. 8000–7500 BCE, that the utilization of interior Scandinavia would have markedly increased, and conequantly a ramping up of human carrying capacity, *sensu* Freeman et al. (2021), could be suggested.

A lag between increased land area and temperature on the one hand, and population size on the other, could be a similar phenomenon as the lagged equilibration processes and human population response to changing climate observed in Bighorn Basin in North American Rocky Mountains (Kelly et al., 2013). The lag in interior Scandinavia before 7500 BCE would in this case be more than 1000 years. The difference between raw bioproductivity and human carrying capacity should maybe be stressed. If the socio-technological strategy employed by the pre-7500 BCE population was not well suited for the utilization of the increased bioproductivity, then the increase did not affect the carrying capacity for humans. A second environmental driver for low population density can in fact be found in the time taken by the environment to develop into a habitable state after ice sheet retreat, a delay that in Fennoscandia has been suggested to have taken 300–900 years (Tallavaara et al., 2014).

5.2. The period of rapid growth after ca. 7500 BCE

From ca. 7500 BCE the developing new inland adaptation resulted in demographic growth in tandem with increasing climatic warming and environmental productivity, until shortly after 6000 BCE when ET (and productivity) started to slowly decrease. The continuously increasing environmentally driven carrying capacity enabled hunter-gatherer population to grow accordingly.

5.3. Population saturation in interior Scandinavia ca. 6000 BCE

Our results suggest that by ca. 6000 BCE the full resource potential for Early Holocene hunter-gatherers was reached in interior Scandinavia and population increase stalled for at least 2000 years. It can be assumed that at this point the area was permanently habitable for a low-density population of terrestrial hunter-gatherers. As indicated by the ET below the 15.25 storage threshold detected in the ethnographic hunter-gatherer data (Binford, 2001, Johnson, 2014), hunter-gatherers at such high latitudes remain highly dependent on the ability to procure a large food surplus during the growing season to get through the winter.

Risks connected to environmental fluctuations grow with population saturation, i.e., when the population size is close to carrying capacity. Negative climatic impacts on productivity, diversity, food availability and pathogen stress become harder to counter, and this is reflected in human population density. As foraging adaptations approach population saturation, land use patterns therefore become more sensitive to decade to century scale climatic variation. This favors social organization and technologies that reduce this sensitivity. Our data is not of such quantity and quality that such patterns could be detected, although they can be assumed. The 8.2 ka climatic event is observable as a downturn in the SPD, but it does not constitute a statistically significant deviation from the logistic growth model.

Freeman et al. (2021: 7–8) suggest that such events with lowered environmental productivity could produce population pressure and thereby promote innovations. Considering the human reproductive potential, and the many episodes of short-lived climatic dowturns probably occurring during the 2000-year interval of stable or slowly decreasing ET, population pressure coupled with a lowered standard of living was probably not a rarity. However, there is no indication in interior Scandinavia of this resulting into innovations to increase carrying capacity, or a ramping up of population density as a consequence of such innovations. Instead, what we see could be either simply a case of predator–prey cycling or a case in which the system flips into what Freeman et al. (2021) call a "poverty trap", i.e., an irreversible cycle in which economic alternatives that appear advantageous in the short run are chosen, leading to a bad situation in the long run because of feedback loops of long-term negative consequences. In this type of development population size can stay close to carrying capacity for extended periods.

Refuse fauna at the interior sites suggests that the hunting of large cervids (Eurasian elk and wild reindeer) played a major role in hunter-gatherer subsistence throughout the Stone Age (Therese Ekholm,

unpublished analysis). This is well in line with the predictions derived from ethnographic hunter-gatherer data. At present, the yield from Eurasian elk (*Alces alces*), red deer (*Cervus elaphus*), and wild reindeer (*Rangifer tarandus*) hunt, as well as from herding of domesticated reindeer, is in the order of some 250,000 animals a year (Supplementary text 4). This is a sustainable harvest and gives an indication of the amount of forage available for cervids in the area. The environment today is somewhat inferior for these animals than 7000 years ago, because spruce forest, a habitat not favorable for cervids, became dominant in the forested parts of the study area during the Late Holocene.

In terms of calories, the amount of cervid meat harvested in the study area today (i.e., ca. 250,000 animals) could theoretically sustain a hunter-gatherer population of roughly 40,000 individuals, if we assume a diet based solely on meat, a way to store meat throughout the year, and consider one animal on average to give 112.5 kg of meat, one kg of raw meat to be 1000 kcal on average, and one person to use 2000 kcal/day. This is a clearly higher population density than could be expected from the low ET values, which suggest large territories and low population density. Even if we do not have any data on absolute population size, we find it likely that the Mesolithic population size in the study area would be in the range of 3750 individuals or 0.75/100 km^2, as modelled by Ordonez and Riede (2022: Fig. 4).

Although it does not consider other means of subsistence, our simple calculation nevertheless shows a clear difference between the potential higher population density from the yield of present day cervid hunting and herding, and the low population density modelled using ethnographic hunter-gatherer data. It suggests that the area potentially could have sustained a far denser population of hunter-gatherers than it did in the Early Holocene, if only there were means to harvest and store more, or to bypass some other limiting factor restricting population growth.

One potential limiting factor was competition. A subsistence system based on large game hunting is largely a predator prey relationship in ecological terms. In such a system the number of prey animals is not determined by the amount of available forage but by predation pressure, as in the classic Lotka–Volterra equation, which produces a pattern of dynamic ups and downs in population size of both predator and prey (Lotka, 1920, Volterra, 1926). Fluctuations in the numbers of Eurasian elk (moose) and wolves on the Isle Royale, documented since 1953, exemplifies this relationship well (Hoy et al., 2022). Over a larger area this can produce a low-density equilibrium (Gasaway et al., 1992), also called "predator pit". Besides humans, the main predators of cervids in Scandinavia are wolves. When humans enter an area, the two combined press down the cervid populations to an even lower density than wolves alone. Even in this situation, the prey population can be maintained on a low-level, if human hunters can access several alternative hunting territories.

From our modern perspective it is easy to note that already in the Mesolithic there were alternatives to increase yields by targeting wolves to reduce competition, by regulating the hunting of cervids according to prey animal sex and age, and by domesticating reindeer - all measures that were applied during later periods and that allowed human population growth. When such measures were not in use, and if hunting of the same cervid stocks was open for all hunters, it became a typical case of the tragedy of the commons (Hardin, 1968). Under such circumstances a hunter should kill all encountered high-ranking prey animals regardless of sex and age, even if just a small proportion of the catch could be utilized. This is because the same animal otherwise would be lost to the hunter and instead killed by another hunter or other predators. Saving an encountered prey animal or protecting the game by reducing the number of wolves, would promote deceivers. We therefore argue, that within a low productivity region like the Scandinavian interior, scattered seasonally rich resources, migrating prey, and low population density, i.e., few people and large territories, made it impossible for Early Holocene groups to control the prey and predator populations enough to allow more efficient sustained harvesting in the long run.

5.4. Environmental or cultural drivers?

In Scandinavia, the marked initial land area growth, coupled with increasing bioproductivity caused by the Early to Middle Holocene warming, resulted in constantly growing bioproductivity until ca. 6000 BCE coupled with a population growth curve resembling logistic growth as it is known in population ecological theory.

According to the MaB-ratchet model (Freeman et al., 2021) logistic population growth among hunter-gatherers is a stepwise sequence of population responses driven by changes in population saturation over time that reflects true short-term episodes of logistic growth. In this model looming population saturation causes technological and/or socioeconomic developments that increase carrying capacity and enable further population growth until population saturation is reached and a new innovation is required to start a new ratchet of logistic growth. The argument by Tallavaara and Jørgensen (2021), that change in carrying capacity was environmentally driven, i.e. not affected by technological and/or socioeconomic changes, does not require cultural drivers to be fulfilled. Instead, hunter-gatherer population will follow the ups and downs in bioproductivity, which in the interior Scandinavian case would result into what we call "false logistic" growth.

Our data suggests that only at the end of the 9500–7500 BCE period, when a permanent interior population started to develop, a ratchet-like increasing of human carrying capacity *sensu* Freeman et al. (2021), could be suggested. The delayed full utilization of the interior, however, could also be a consequence of a lagged human population response to changing climate and/or a delay caused by the time needed for the environment to develop after ice sheet retreat. After the first 2000 to 1500 years, rapid population growth took place in tandem with the warming climate, while the growth was stalled only by the end of the Holocene Thermal Maximum. After ca. 6000 BCE a 2000-year long phase of stable or slowly decreasing population followed. Since during the ca. 8000–4000 BCE period we detect no such changes in hunter-gatherer subsistence technology that could be seen as markedly increasing human carrying capacity, we argue that what we see in Early to Mid-Holocene interior Scandinavia is "false logistic" growth driven by changes in the environmentally driven carrying capacity in a low productivity environment.

6. Conclusions

To conclude, some wider implications for the dates-as-data method should be pointed out. First, the study underlines the fact that when employing summed probability distributions of radiocarbon dates to study human population dynamics, an exponential increase in the number of dates with time should not be assumed. Instead, the null model with the best fit with the respective radiocarbon date dataset should be sought for and selected, be it exponential, linear, logistic, or constant growth. Second, our results suggest that in early postglacial low productivity environments hunter-gatherer datasets can be expected to fit a logistic growth curve due to changing carrying capacity causing "false logistic" growth, i.e., a demographic development in which population growth follows from increasing carrying capacity before being stalled by environmental constraints inherent in low productivity regions.

CRediT authorship contribution statement

Mikael A. Manninen: Conceptualization, Methodology, Formal analysis, Investigation, Data curation, Writing – original draft, Writing – review & editing. **Guro Fossum:** Conceptualization, Methodology, Investigation, Resources, Data curation, Writing – original draft. **Therese Ekholm:** Conceptualization, Methodology, Investigation, Resources, Data curation, Writing – original draft. **Per Persson:** Conceptualization, Methodology, Software, Formal analysis, Investigation, Resources, Data curation, Writing – original draft, Writing – review &

editing, Visualization, Supervision.

Declaration of Competing Interest

The authors declare that they have no known competing financial interests or personal relationships that could have appeared to influence the work reported in this paper.

Acknowledgements

The authors wish to thank two anonymous reviewers for their helpful comments on an earlier draft of the paper. We also thank Michel Guinard, Department of Archaeology and Ancient History, Uppsala University, Sweden, for giving access to his unpublished database of radiocarbon dates, as well as Tom Carlsson, Stiftelsen Kulturmiljövård, Sweden, Ellen Friis, Museum of Cultural History, University of Oslo, Norway, Hans Olsson, Värmlands Museum, Sweden, and Joakim Wehlin, Dalarnas Museum, Sweden, for letting us use their previously unpublished radiocarbon dates.

Funding.

This work was supported by the Kone Foundation, Helsinki, Finland, project 202007450.

Appendix A. Supplementary data

Supplementary data to this article can be found online at https://doi.org/10.1016/j.jaa.2023.101497.

References

Agerskov Rose, H., Meadows, J., Palstra, S.V.L., Hamann, C., Boudin, M., Huels, M., 2019. Radiocarbon Dating Cremated Bone: A Case Study Comparing Laboratory Methods. Radiocarbon 61 (5), 1581–1591. https://doi.org/10.1017/RDC.2019.70.

Alley, R.B., Mayewski, P.A., Sowers, T., Stuiver, M., Taylor, K.C., Clark, P.U., 1997. Holocene climate instability: a prominent, widespread event 8200 yr ago. Geology 25, 483–546. https://doi.org/10.1130/0091-7613(1997)025<0483:HCIAPW>2.3.CO;2.

Antonsson, K., Seppä, H., 2007. Holocene temperatures in Bohuslän, southwest Sweden: a quantitative reconstruction from fossil pollen data. Boreas 36 (4), 400–410. https://doi.org/10.1080/03009480701317421.

Aune, B., 1993. *Air temperature normals, normal period 1961-1990*. Norwegian Meterological Institute Report Climate 2/1993.

Bailey, H.P., 1960. A Method of Determining the Warmth and Temperateness of Climate. Geografiska Annaler 42 (1), 1–16.

Bailey, R.G., 2014. Ecoregions. The Ecosystem Geography of the Oceans and Continents, Springer, New York - Heidelberg - Dordrecht - London.

Bang-Andersen, S., 2012. Colonizing contrasting landscapes. The pioneer coast settlement and inland utilization in southern norway 10,000–9500 years before present. Oxford Journal of Archaeology 31 (2), 103–120. https://doi.org/10.1111/j.1468-0092.2012.00381.x.

Bang-Andersen, S., 2013. Human exploitation of Southwest Norwegian mountains during the Mesolithic (ca. 9800–5700 y.BP): research history, trends, challenges. Preistoria Alpina 47, 69–75.

Bang-Andersen, S., 1990. The Myrvatn Group, a Preboreal Find-Complex in South-west Norway, in: Vermeersch, P.M., Van Peer, P. (Eds.), Contributions to the Mesolithic in Europe. *Studia Praehistoria Belgica V*, 215–25.

Begon, M., Harper, J.L., Townsend, C.R., 1996. Ecology. Individuals, Populations and Communities, Third edition. Blackwell Science, Oxford.

Bevan, A., Colledge, S., Fuller, D., Fyfe, R., Shennan, S., Stevens, C., 2017. Holocene fluctuations in human population demonstrate repeated links to food production and climate. Proceendings of the National Academy of Sciences 114 (49), E10524–E10531. https://doi.org/10.1073/pnas.1709190114.

Binford, L.R., 1980. Willow smoke and dogs' tails: Hunter-gatherer settlement systems and archaeological site formation. American Antiquity 45, 4–20. https://doi.org/10.2307/279653.

Binford, L.R., 2001. Constructing Frames of Reference. An Analytical Method for Archaeological Theory Building Using Ethnographic and Environmental Data Sets. University of California Press, Berkeley.

Boaz, J., 1999. Pioneers in the Mesolithic: The initial Occupation of the interior of Eastern Norway. In Boaz, J. (Ed.) *The Mesolithic of Central Scandinavia*. (125–52). Universitetets Oldsaksamlings Skrifter. Ny Rekke 22. Oslo.

Boethius, A., Ahlström, T., 2018. Fish and resilience among Early Holocene foragers of southern Scandinavia: A fusion of stable isotopes and zooarchaeology through Bayesian mixing modelling. Journal of Archaeological Science 93, 196–210. https://doi.org/10.1016/j.jas.2018.02.018.

Boserup, E., 1965. The Condition of Agricultural Growth: The Economics of Agrarian Change under Population Pressure. Allen and Unwin, London.

Breivik, H.M., Callanan, M., 2016. Hunting High and Low: Postglacial Colonization Strategies in Central Norway between 9500 and 8000 cal BC. European Journal of Archaeology 19 (4), 571–595. https://doi.org/10.1080/14619571.2016.1147315.

Broughton, J.M., Weitzel, E.M., 2018. Population reconstructions for humans and megafauna suggest mixed causes for North American Pleistocene extinctions. Nature Communications 9, 5441. https://doi.org/10.1038/s41467-018-07897-1.

Brown, W.A., 2015. Through a filter, darkly: Population size estimation, systematic error, and random error in radiocarbon-supported demographic temporal frequency analysis. Journal of Archaeological Science 53, 133–147. https://doi.org/10.1016/j.jas.2014.10.013.

Brown, A.A., Crema, E.R., 2019. Māori Population Growth in Pre-contact New Zealand: Regional Population Dynamics Inferred From Summed Probability Distributions of Radiocarbon Dates. The Journal of Island and Coastal Archaeology 16 (2–4), 572–590. https://doi.org/10.1080/15564894.2019.1605429.

Contreras, D., Meadows, J., 2014. Summed radiocarbon calibrations as a population proxy: A critical evaluation using a realistic simulation approach. Journal of Archaeological Science 52, 591–608. https://doi.org/10.1016/j.jas.2014.05.030.

Couillard, P.-L., Tremblay, J., Lavoie, M., Payette, S., 2019. Comparative methods for reconstructing fire histories at the stand scale using charcoal records in peat and mineral soils. Forest Ecology and Management 433, 376–385. https://doi.org/10.1016/j.foreco.2018.11.015.

Crema, E.R., 2022. Statistical Inference of Prehistoric Demography from Frequency Distributions of Radiocarbon Dates: A Review and a Guide for the Perplexed. Journal of Archaeological Method and Theory 2022. https://doi.org/10.1007/s10816-022-09559-5.

Crema, E.R., Bevan, A., 2021. Inference from large sets of radiocarbon dates: software and methods. Radiocarbon 63 (1), 23–39. https://doi.org/10.1017/RDC.2020.95.

Crema, E.R., Habu, J., Kobayashi, K., Madella, M., 2016. Summed Probability Distribution of ^{14}C Dates Suggests Regional Divergences in the Population Dynamics of the Jomon Period in Eastern Japan. PLoS ONE 11 (4), e0154809.

Crombé, P., Robinson, E., 2014. C-14 dates as demographic proxies in Neolithisation models of northwestern Europe: a critical assessment using Belgium and northeast France as a case-study. Journal of Archaeological Science 52, 558–566. https://doi.org/10.1016/j.jas.2014.02.001.

Crombé, P., Boudin, M., Van Strydonck, M., 2021. Can calcined bones be used to date Final Palaeolithic and Mesolithic open-air sites? A case-study from the Scheldt basin (NW Belgium). Journal of Archaeological Science 131, 105411. https://doi.org/10.1016/j.jas.2021.105411.

Damlien, H., Solheim, S., 2018. The pioneer settlement of Eastern Norway. In: Blankholm, H.P. (Ed.), *Early Economy and Settlement in Northern Europe, Pioneering, Resource Use, Coping with Change*. Early Settlement of Northern Europe, 3. Equinox, Sheffield, pp. 335–367.

Daniels, J., 2010. Paleogeographical maps and visualisation of shore-level changes. Unpublished digital atlas, Sveriges geologiska undersökning.

Ekholm, T. 2015. A cross-check of radiocarbon dates from Stone Age Sites in Northern Sweden. *Fornvännen* 110, 127–140. urn:nbn:se:raa:diva-2701.

Fernández-López de Pablo, J., Gutiérrez-Roig, M., Gómez-Puche, M., McLaughlin, R., Silva, F., Lozano, S., 2019. Palaeodemographic modelling supports a population bottleneck during the Pleistocene-Holocene transition in Iberia. Nature Communications 10, 1872. https://doi.org/10.1038/s41467-019-09833-3.

Ficetola, F.G., Marta, S., Guerrieri, A., Gobbi, M., Ambrosini, R., Fontaneto, D., Zerboni, A., Poulenard, J., Caccianiga, M., Thuiller, W., 2019. Dynamics of Ecological Communities Following Current Retreat of Glaciers. Annual Review of Ecology, Evolution, and Systematics 52, 405–426. https://doi.org/10.1146/annurev-ecolsys-010521-040017.

Fischer, A.G., 1960. Latitudinal variations in organic diversity. Evolution 14 (1), 64–81. https://doi.org/10.1111/j.1558-5646.1960.tb03057.x.

Freeman, J., Hard, R.J., Mauldin, R.P., Anderies, J.M., 2021. Radiocarbon data may support a Malthus-Boserup model of hunter-gatherer population expansion. Journal of Anthropological Archaeology 63, 101321. https://doi.org/10.1016/j.jaa.2021.101321.

Gamble, C., Davies, W., Pettitt, P., Hazelwood, L., Richards, M., 2005. The archaeological and genetic foundations of the European population during the Late Glacial: implications for 'agricultural thinking'. Cambridge Archaeological Journal 15 (2), 193–223. https://doi.org/10.1017/S0959774305000107.

Gasaway, W.C., Boertje, R.D., Grangaard, D.V., Kelleyhouse, D.G., Stephenson, R.O., Larsen, D.G., 1992. The role of predation in limiting moose at low densities in Alaska and Yokon and implications for conservation. Wildlife Monographs 120, 1–59.

Goldberg, A., Mychajliw, A.M., Hadly, E.A., 2016. Post-invasion demography of prehistoric humans in South America. Nature 532, 232–235. https://doi.org/10.1038/nature17176.

Hardin, G., 1968. The Tragedy of the Commons. Science 162 (3859), 1243–1248. https://doi.org/10.1126/science.162.3859.124.

Hoy, S.R., Peterson, R.O., Vucetich, J.A., 2022. Ecological Studies of Wolves on Isle Royale, Annual Report 2021–2022. Michigan Technological University, Houghton, College of Forest Resources and Environmental Science.

Johnson, A.L., 2014. Exploring Adaptive Variation among Hunter-gatherers with Binford's Frames of Reference. Journal of Archaeological Research 22, 1–42. https://doi.org/10.1007/s10814-013-9068-y.

Jørgensen, E.K., 2018. The palaeodemographic and environmental dynamics of prehistoric Arctic Norway: An overview of human-climate covariation. Quaternary International 549, 36–51. https://doi.org/10.1016/j.quaint.2018.05.014.

Jørgensen, E.K., Pesonen, P., Tallavaara, M., 2022. Synchronous human population dynamics and adaptive strategies among early and mid-Holocene coastal hunter-gatherers in Northern Europe. Quarternary Research 108, 107–122. https://doi.org/10.1017/qua.2019.86.

Kelly, R.L., 1983. Hunter-Gatherer Mobility Strategies. Journal of Anthropological Research 39 (3), 277–306. https://doi.org/10.1086/jar.39.3.3629672.
Kelly, R.L., 2013. The Lifeways of Hunter-Gatherers: The Foraging Spectrum. Cambridge University Press, Cambridge.
Kelly, R.L., Surovell, T.A., Shuman, B.N., Smith, G.M., 2013. A continuous climatic impact on Holocene human population in the Rocky Mountains. *Proceedings of the National Academy of Sciences* 110, 443–7. https://doi.org/10.1073/pnas.1201341110.
Kingsland, S., 1982. The Refractory Model: The Logistic Curve and the History of Population Ecology. The Quarterly Review of Biology 57 (1), 29–52. https://doi.org/10.1086/412574.
Lanting, J.N., Brindley, A.L., 1998. Dating cremated bone: the dawn of a new era. Journal of Irish Archaeology 9, 1–7.
Lanting, J.N., Aerts-Bijma, A.T., van der Plicht, J., 2001. Dating of cremated bones. Radiocarbon 43 (2A), 249–254. https://doi.org/10.1017/S0033822200038078.
Lilleøren, K.S., Etzelmüller, B., Schuler, T.V., Gisnås, K., Humlum, O., 2012. The relative age of mountain permafrost – estimation of Holocene permafrost limits in Norway. Global and Planetary Change 209–223. https://doi.org/10.1016/j.gloplacha.2012.05.016.
Lohne, O.S., Mangerud, J., Birks, H.H., 2013. Precise ^{14}C ages of the Vedde and Saksunarvatn ashes and the Younger Dryas boundaries from western Norway and their comparison with the Greenland Ice Core (GICC05) chronology. Journal of Quaternary Science 28, 490–500. https://doi.org/10.1002/jqs.2640.
Lotka, A. J., 1920. Analytical Note on Certain Rhythmic Relations in Organic Systems. *Proceedings of the National Academy of Sciences* 6(7), 410–5. https://doi.org/10.1073/pnas.6.7.410.
Malthus, T.R., 1798.. An Essay on the Principle of Population as it Affects the Future Improvement of Society. J. Johnson, London.
Manninen, M.A., Tallavaara, M., Seppä, H., 2018. Human responses to early Holocene climate variability in eastern Fennoscandia. Quaternary International 465, 287–297. https://doi.org/10.1016/j.quaint.2017.08.043.
Manninen, M.A., Damlien, H., Kleppe, J.I., Knutsson, K., Murashkin, A., Niemi, A.R., Rosenvinge, C.S., Persson, P., 2021. First encounters in the north: Cultural diversity and gene flow in Early Mesolithic Scandinavia. Antiquity 95 (380), 310–328. https://doi.org/10.15184/aqy.2020.252.
Mansrud, A., Persson, P., 2018. Waterworld: Environment, Animal Exploitation, and Fishhook Technology in the North-Eastern Skagerrak Area During the Early and Middle Mesolithic (9500–6300 cal BC). In: Persson, P., Riede, F., Skar, B., Jonsson, L. (Eds.), The Ecology of Early Settlement in Northern Europe. Equinox Publishing, Bristol, pp. 129–165.
Melvold, S., 2011. Råstoff og kommunikasjon i pionerfasen ved Rena elv. Primitive tider 13, 47–59.
Naysmith, P., Scott, E.M., Cook, G.T., Heinemeier, J., van der Plicht, J., van Strydonck, M., Bronk Ramsey, C., Grootes, P.M., Freeman, S.P.H.T., 2007. A Cremated Bone Intercomparison Study. Radiocarbon 49 (2), 403–408. https://doi.org/10.1017/S0033822200042338.
Nesje, A., Dahl, S.O., 2001. The Greenland 8200 cal. yr BP event detected in loss-on-ignition profiles in Norwegian lacustrine sediment sequences. Journal of Quaternary Science 16, 155–166. https://doi.org/10.1002/jqs.567.
Nielsen, S.V., 2021. Late Mesolithic forager dispersal caused pre-agricultural demographic transition in Norway. Oxford Journal of Archaeology 40, 153–175.
Nielsen, S.V., Persson, P., Solheim, S., 2019. De-Neolithisation in southern Norway inferred from statistical modelling of radiocarbon dates. Journal of Anthropological Archaeology 53, 82–91. https://doi.org/10.1016/j.jaa.2018.11.004.
Oinonen, M., Hertell, E., Mannermaa, K., Manninen, M.A., Tallavaara, M. & Pesonen, P. 2013. *Archaeological burnt bone dates in eastern Fennoscandia*. Poster presented at the 14C & archaeology conference, Ghent, Belgium 8–12.4. 2013. https://doi.org/10.13140/RG.2.1.2023.4727.
Olsen, J., Heinemeier, J., Hornstrup, K.M., Bennike, P., Thrane, H., 2013. 'Old wood' effect in radiocarbon dating of prehistoric cremated bones? Journal of Archaeological Science 40 (1), 30–34. https://doi.org/10.1016/j.jas.2012.05.034.
Ordonez, A., Riede, F., 2022. Changes in limiting factors for forager population dynamics in Europe across the last glacial-interglacial transition. Nature Communications 13, 5140. https://doi.org/10.1038/s41467-022-32750-x.
Palmisano, A., Bevan, A., Shennan, S., 2017. Comparing archaeological proxies for long-term population patterns: An example from central Italy. Journal of Archaeological Science 87, 59–72. https://doi.org/10.1016/j.jas.2017.10.001.
Palmisano, A., Lawrence, D., de Gurchy, M.V., Bevan, A., Shennan, S., 2021. Holocene regional population dynamics and climatic trends in the Near East: A first comparison using archaeo-demographic proxies. Quaternary Science Reviews 252, 106739. https://doi.org/10.1016/j.quascirev.2020.106739.
Påsse, T., J. Daniels, J., 2011. "Comparison between a new and an old semiempirical Fennoscandian shore-level model." In Ikonen, A. and Lipping, T. (eds.) *Proceedings of a Seminar on Sea Level Displacement and Bedrock Uplift*, 10–11 June 2010. (47–50) Pori: Posiva.
Påsse, T., Andersson, L., 2005. Shore-level displacement in Fennoscandia calculated from empirical data. GFF 127 (4), 253–268. https://doi.org/10.1080/11035890501274253.
Reimer, P., Austin, W., Bard, E., Bayliss, A., Blackwell, P., Bronk Ramsey, C., Butzin, M., Cheng, H., Edwards, R., Friedrich, M., Grootes, P., Guilderson, T., Hajdas, I., Heaton, T., Hogg, A., Hughen, K., Kromer, B., Manning, S., Muscheler, R., Palmer, J., Pearson, C., van der Plicht, J., Reimer, R., Richards, D., Scott, E., Southon, J., Turney, C., Wacker, L., Adolphi, F., Büntgen, U., Capano, M., Fahrni, S., Fogtmann-Schulz, A., Friedrich, R., Köhler, P., Kudsk, S., Miyake, F., Olsen, J., Reinig, F., Sakamoto, M., Sookdeo, A., Talamo, S., 2020. The IntCal20 Northern Hemisphere radiocarbon age calibration curve (0–55 cal kBP). Radiocarbon 62, 725–757. https://doi.org/10.1017/RDC.2020.41.
Rick, J.W., 1987. Dates as data: an examination of the Peruvian Preceramic radiocarbon record. American Antiquity 52, 55–73. https://doi.org/10.2307/281060.
Riede, F., 2009. Climate and demography in early prehistory: using calibrated (14)C dates as population proxies. *Human Biology* 81 (3), 309–337. https://doi.org/10.3378/027.081.0311.
Roberts, N., Woodbridge, J., Bevan, A., Palmisano, A., Shennan, S., Asouti, E., 2018. Human responses and non-responses to climatic variations during the last Glacial-Interglacial transition in the eastern Mediterranean. Quaternary Science Reviews 184, 47–67. https://doi.org/10.1016/j.quascirev.2017.09.011.
Rockwood, L.L., 2006. Introduction to Population Ecology. Blackwell Publishing, Malden.
Schulting, R.J., Mannermaa, K., Tarasov, P.E., Higham, T., Bronk Ramsey, C., Khartanovich, V., Moiseyev, V., Gerasimov, D., O'Shea, J., Weber, A., 2022. Radiocarbon dating from Yuzhniy Oleniy Ostrov cemetery reveals complex human responses to socio-ecological stress during the 8.2 ka cooling event. Nature Ecology & Evolution 6, 155–162. https://doi.org/10.1038/s41559-021-01628-4.
Seppä, H., Hammarlund, D., Antonsson, K., 2005. Low-frequency and high-frequency changes in temperature and effective humidity during the Holocene in south-central Sweden: implications for atmospheric and oceanic forcings of climate. Climate Dynamics 25, 285–297. https://doi.org/10.1007/s00382-005-0024-5.
Shennan, S., Edinborough, K., 2007. Prehistoric population history: from the Late Glacial to the Late Neolithic in Central and Northern Europe. Journal of Archaeological Science 34 (8), 1339–1345. https://doi.org/10.1016/j.jas.2006.10.031.
Shennan, S., Sear, R., 2021. Archaeology, demography and life history theory together can help us explain past and present population patterns. Philosophical Transactions of the Royal Society B 376 (1816), 20190711. https://doi.org/10.1098/rstb.2019.0711.
Shennan, S., Downey, S.S., Timpson, A., Edinborough, K., Colledge, S., Kerig, T., Manning, K., Thomas, M.G., 2013. Regional population collapse followed initial agriculture booms in mid-Holocene Europe. *Nature*. Communications 4, ncomms3486. https://doi.org/10.1038/ncomms3486.
Skar, B., Lidèn, K., Eriksson, C., Sellevold, B., 2016. A submerged Mesolithic grave site reveals remains of the first Norwegian seal hunters. In Bjerck, H.B., Breivik, H.M., Fretheim, S., Piana, E.L., Skar, B., Tivoli, A.M., Zangrando, A.F. (Eds.) *Marine Ventures. Archaeological Perspectives on Human-Sea Relations. Proceedings from the Marine Ventures International Symposium in Trondheim 2013.* (225–39). Sheffield: Equinox.
Solheim, S., 2020. Mesolithic coastal landscapes. Demography, settlement patterns and subsistence economy in southeastern Norway. In: Schülke, A. (Ed.), Coastal Landscapes of the Mesolithic. Human Engagement with the Coast from the Atlantic to the Baltic Sea. Routledge, London, pp. 44–74.
Solheim, S., Persson, P., 2018. Early and mid-Holocene coastal settlement and demography in southeastern Norway: Comparing distribution of radiocarbon dates and shoreline-dated sites, 8500–2000 cal. BCE. *Journal of Archaeological Science: Reports* 19, 334–343. https://doi.org/10.1016/j.jasrep.2018.03.007.
Stroeven, A.P., Hättestrand, C., Kleman, J., Heyman, J., Fabel, D., Fredin, O., Goodfellow, B.W., Harbor, J.M., Jansen, J.D., Olsen, L., Caffee, M.W., Fink, D., Lundqvist, J., Rosqvist, G.C., Strömberg, B., Jansson, K.N., 2016. Deglaciation of Fennoscandia. Quaternary Science Reviews 147, 91–121. https://doi.org/10.1016/j.quascirev.2015.09.016.
Surovell, T.A., Finley, J., Smith, G.M., Brantingham, P.J., Kelly, R., 2009. Correcting temporal frequency distributions for taphonomic bias. Journal of Archaeological Science 36 (8), 1715–1724. https://doi.org/10.1016/j.jas.2009.03.029.
Tallavaara, M., 2015. Humans under climate forcing: How climate change shaped hunter-gatherer population dynamics in Europe 30,000–4000 years ago. Unigrafia, Helsinki.
Tallavaara, M., Manninen, M.A., Pesonen, P., Hertell, E., 2014. Radiocarbon dates and postglacial colonisation dynamics in eastern Fennoscandia. In Riede, F., Tallavaara, M. (eds.) *Lateglacial and Postglacial Pioneers in Northern Europe*. (161–75) British Archaeological Reports, International Series S2599.
Tallavaara, M., Eronen, J.T., Luoto, M., 2018. Productivity, biodiversity, and pathogens influence the global hunter-gatherer population density. *Proceedings of the National Academy of Sciences* 115(6), 1232–37. https://doi.org/10.1073/pnas.1715638115.
Tallavaara, M., Jørgensen, E.K., 2021. Why are population growth rate estimates of past and present hunter–gatherers so different? *Philosophical Transactions of the Royal Society* B376, 20190708. https://doi.org/10.1098/rstb.2019.0708.
Tallavaara, M., Seppä, H., 2012. Did the mid-Holocene environmental changes cause the boom and bust of hunter-gatherer population size in eastern Fennoscandia? The Holocene 22 (2), 215–225. https://doi.org/10.1177/0959683611414.
Timpson, A., Colledge, S., Crema, E., Edinborough, K., Kerig, T., Manning, K., Thomas, M.G., Shennan, S., 2014. Reconstructing regional population fluctuations in the European Neolithic using radiocarbon dates: a new case-study using an improved method. Journal of Archaeological Science 52, 549–557. https://doi.org/10.1016/j.jas.2014.08.011.
Torfing, T., 2015. Neolithic population and summed probability distribution of 14 C-dates. Journal of Archaeological Science 63, 193–198. https://doi.org/10.1016/j.jas.2015.06.004.
Tørhaug, V., Åstveit, L.I., 2000. Steinalderboplassene ved Store Fløyrlivatn. Frá haug ok heiðni 1 (2000), 35–39.
van Strydonck, M., Boudin, M., De Mulder, G., 2009. 14C Dating of Cremated Bones: The Issue of Sample Contamination. Radiocarbon 51 (2), 553–568. https://doi.org/10.1017/S0033822200055922.
Verhulst, P.-F., 1838. Notice sur la loi que la population suit dans son accroissement. Correspondance mathématique et physique 10, 113–121.

Virtanen, R., Oksanen, L., Oksanen, T., Cohen, J., Forbes, B.C., Johansen, B., Käyhkö, J., Olofsson, J., Pulliainen, J., Tømmervik, H., 2016. Where do the treeless tundra areas of northern highlands fit in the global biome system: toward an ecologically natural subdivision of the tundra biome. Ecology and Evolution 6 (1), 143–158. https://doi.org/10.1002/ece3.1837.

Volterra, V., 1926. Variazioni e fluttuazioni del numero d'individui in specie animali conviventi. Memorie della Reale Accademia Nazionale dei Lincei 2, 31–113.

Williams, A.N., 2012. The use of summed radiocarbon probability distributions in archaeology: a review of methods. Journal of Archaeological Science 39, 578–589. https://doi.org/10.1016/j.jas.2011.07.014.

Wood, J.W., 1998. A Theory of Preindustrial Population Dynamics Demography, Economy, and Well-Being in Malthusian Systems. Current Anthropology 39 (1), 99–135. https://doi.org/10.1086/204700.

Zahid, H.J., Robinson, E., Kelly, R.L., 2016. Agriculture, population growth, and statistical analysis of the radiocarbon record. Proceedings of the National Academy of Sciences 113, 931–935. https://doi.org/10.1073/pnas.1517650112.

Zhu, D., Galbraith, E.D., Reyes-García, V., Ciais, P., 2021. Global hunter-gatherer population densities constrained by influence of seasonality on diet composition. Nature Ecology and Evolution 5, 1536–1545. https://doi.org/10.1038/s41559-021-01548-3.